Journal of Applied Sciences and Nanotechnology, Vol. 2, No. 4 (2022)

Journal of Applied Sciences and Nanotechnology

Journal homepage: https://jasn.uotechnology.edu.iq/

Recent Advances to Overcome Methane Hydrate Formation Challenges Using Nanostructure Promoters: A Mini Review towards Industrialization

Mohsen Hosseini*

Department of Chemical Engineering, Virginia Polytechnic Institute and State University – United States

Article information

Article history:

Received: January, 26, 2022

Accepted: February, 27, 2022

Available online: December, 10, 2022

Keywords:

Methane,

Hydrate,

Nanostructure promoters

Corresponding Author:

Mohsen Hosseini

mohsenhosseini@vt.edu

Abstract

Natural gas has recently drawn considerable attention due to its low emissions upon combustion. Pipeline transmission of natural gas is costly and always encounters different obstacles. Therefore, an effective industrial alternative for the storage and transmission of natural gas is needed. Hydrates, also known as solidified natural gas, have been proven to be a more feasible replacement compared to pipeline transmission, CNG, or LNG. Scientists have introduced promoters to shorten the induction time, increase the storage capacity, and improve the stability of hydrates. Nanostructure materials have demonstrated promising promotion results, suggesting a bright future and a critical step in the industrialization of this technology. Researchers have mainly used pure methane, which is the main component of natural gas, to form hydrates. In this article, the fundamentals of the selection of a nanopromoter, the hydrate formation process, and related calculations are demonstrated. Finally, recent results have been brought together to provide an overview of advances towards the use of nanostructure promoters to tune hydrates for future industrial processes.

DOI: 10.53293/jasn.2022.4676.1133, Department of Applied Sciences, University of Technology

1. Introduction

Methane is one of the main sources of energy and the primary component of natural gas. The formation of gas hydrates is not generally favored in the transmission of natural gas through pipelines [1]. In fact, hydrate inhibitors are usually injected into the gas stream to mitigate the risk of clogging the pipeline [2]. However, significant progress has been made in the last decade to make use of hydrates by encapsulating gases, especially methane, and using them as energy sources [3, 4]. This process enables methane to be stored efficiently at temperatures above the freezing point of water and pressures near atmospheric conditions. The maximum amount of methane storage in the form of natural gas has been estimated to be as high as 180 $\text{Volume}_{\text{gas}}/\text{Volume}_{\text{hydrate}}$ [5-7], making this method a worthy competitor for CNG or LNG [8, 9]. Methane and water are the main constituents of methane hydrates. When they are introduced into a system at high pressure and near the water’s freezing point temperature, ice-like crystalline hydrates are formed. Upon the formation of hydrates, the pressure can be reduced to atmospheric pressure and methane hydrates can be collected. During the pressure reduction, methane hydrates tend to exhibit a self-preservation property [10, 11] that protects them against gas slip or dissociation. Self-preservation is a phenomenon in which hydrates begin to dissociate and create a small amount of water melt which will freeze around the crystals immediately and act as a layer of insulation. This insulation avoids the efficient heat transfer needed to dissociate the remaining hydrates and make them able to retain their crystalline structure at atmospheric pressure. Another phenomenon, the thermal history of the water, also contributes to the use of hydrates as energy carriers. It has been proven that the period of nucleation in water is decreased when water is kept near its freezing point [12]. The same phenomenon has also been reported for natural gas [13] and is known as the memory effect [14, 15]. The memory effect reduces the induction time when a liquid phase is repeatedly used in a gas hydrate formation process. The formation of methane hydrates in the presence of pure water has demonstrated obstacles, such as the slow rate of hydrate formation, relatively low stability of hydrates, and the limited amount of gas storage capacity[16, 17]. One of the main reasons for this could be the extremely small quantity of homogeneous hydrate nucleation in the absence of promoters [18]. In this connection, scientists have started introducing hydrate formation promoters to overcome the foregoing difficulties. Promoters are certain chemicals that are added to water in small quantities to alter the system’s properties. The promoted properties of the fluid improve the characteristics and facilitate the formation of hydrates. The new properties either thermodynamically change the condition of hydrate formation to new moderate pressure and temperature (thermodynamic promoter) or facilitate the process by upgrading the system properties (Kinetic promoter). Surfactants have been widely studied [19-21] as potential thermodynamic promoters due to their ability to modify the interfacial interactions, and researchers have shown that methane storage capacity is considerably increased in the presence of hydrophilic surfactants such as Cetyl Trimethyl Ammonium Bromide (CTAB) [22, 23], Tetrahydrofuran (THF) [24-26] and Sodium dodecyl sulfate (SDS) [19, 20, 27]. The use of jacketed reactor, agitation[28], spraying[29], and bubbling[30] are popular kinetic promoters that are widely used in studies. Another novel approach to promote the hydrate formation process is to use a porous system, where hydrates grow within the porosity [31, 32]. Coolants are used in jacketed reactors to decrease the reactor temperature since the hydrate formation reaction is an exothermic reaction and efficient reduction of the heat from the system is necessary for maximum conversion. Additionally, agitation will introduce turbulence into the system and improve the availability of reactants to participate in the reaction. Nanostructure materials have drawn a lot of attention in hydrate formation processes in recent years due to the unique characteristics that they can introduce into the system. Nanomaterials are usually added to water as a kinetic promoter to yield a uniform nanofluid with promoted characteristics compared to pure water. This addition has been proven to efficiently promote the hydrate formation process as they can improve the heat transfer [33] within the reactor as well as provide high surface-to-volume nucleation active sites, which is favored in the nucleation step [34]. In this mini-review paper, we demonstrate the fundamentals of hydrate formation apparatus and calculation and then focus on the recent uses of nanostructured materials and their impact on the hydrate formation of methane and natural gas.

2. Theoretical Section: Apparatus, Fundamentals and General Calculations

Methane hydrates are typically formed at very high pressures, while low temperatures can assist the formation of hydrates [35]; therefore, temperatures near the freezing point of water are usually selected for the reaction. Figure 1 shows a simplified schematic of a hydrate formation apparatus. Temperature and pressure of the reactor as well as the speed of the agitator are collected and recorded over time using precise instruments. Methane gas should be brought into contact with water/promoter solution under certain mechanical and thermodynamic conditions for hydrates to form. Initially, the reactor is thoroughly washed and rinsed repeatedly with ethanol and DI water and dried to ensure that the reaction chamber does not contain any dust, debris, or other dissolution/nucleation interfering parameter. Then, the reactor is charged with water/promoter solution. Subsequently, methane at a regulated pressure is introduced to purge any trapped gas and fill the reactor. Mechanical/magnetic agitation is also employed, and the coolant circulator valve is opened to allow the reactor temperature to decrease until it reaches the set point. A high-pressure jacketed reactor is the heart of the apparatus. The analysis of the change of the reactor pressure over time is highly useful and provides valuable kinetic and thermodynamic insights. Typically, a slight drop in the pressure of the system occurs initially, which can be attributed to the partial dissolution of gas into water/promoter solution. Subsequently, the pressure of the reactor remains unchanged for relatively a long period. This period is known as induction time and is the time needed for the dissolved gas to create initial nuclei at homogenous and heterogeneous sites [36, 37]. Induction time also represents the period that a supersaturated system can remain in a metastable condition [38, 39]. This time is inversely related to the tendency of a system to create homogenous nuclei that are the result of the initial dissolution of methane in the liquid phase. Following the induction time, clathrate hydrates start to form and a sharp decrease in the reactor pressure is observed. This pressure drop continues until the system reaches a thermodynamic equilibration.

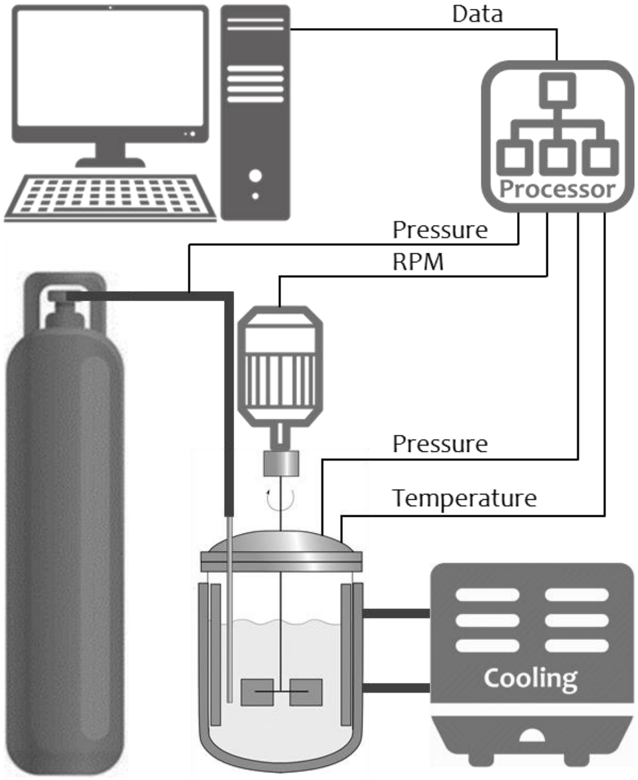

Figure 1. A typical apparatus used for hydrate formation process.

Figure 2 (drawn and modified after work done by Pasieka et al. [40]) demonstrates a schematic of three stages of a typical hydrate formation process. The amount of gas present in the reactor at each time can be calculated by adding the compressibility factor Z to the equation of state.

$$n = \frac{PV}{ZRT} \tag{1}$$

Where n, P, V, R, and T are the number of moles, pressure of the reactor, free volume of the reactor, the gas constant, and the temperature of the reactor respectively. Using Eq. (1), the difference of the mole value of methane at any time compared to the initial value can be calculated and used to determine the amount of hydrated gas. This value can also be used to calculate the storage capacity of hydrates, which is the volume of the hydrated gas at standard conditions divided by the volume of hydrates. Storage capacity for gas hydrates can be calculated using Eq. (2) [41, 42], Where n, V_{mw}, V_{mg}, V_w, and ΔV are the number of moles of hydrated gas, molar volume of water at STP, molar volume of gas at STP and the difference of molar volume of water and hydrate of gas respectively.

$$V/V_{Hyd} = \frac{n\,V_{mw}\,V_{mg}}{V_w\,(V_{mw} + \Delta V)} \tag{2}$$

For methane hydrates, after substituting the values according to the literature [43], Eq. (3) is generated which can directly calculate the storage capacity of methane hydrates, where n and V_w dimensions are mole and cm^3 respectively.

$$V/V_{Hyd} = 20750.93\left(\frac{n}{V_w}\right) \tag{3}$$

To conduct stability studies on hydrates, the temperature of the reactor is decreased to below the freezing temperature of the water and maintained at that temperature for several hours [6, 44]. Next, the unreacted methane gas is vented from the reactor until the pressure of the reactor drops to atmospheric pressure. Subsequently, the relief valve is closed, cooling is stopped, and the pressure of the reactor is studied over time to obtain the percentage of dissociation of methane hydrates using Eq. (1).

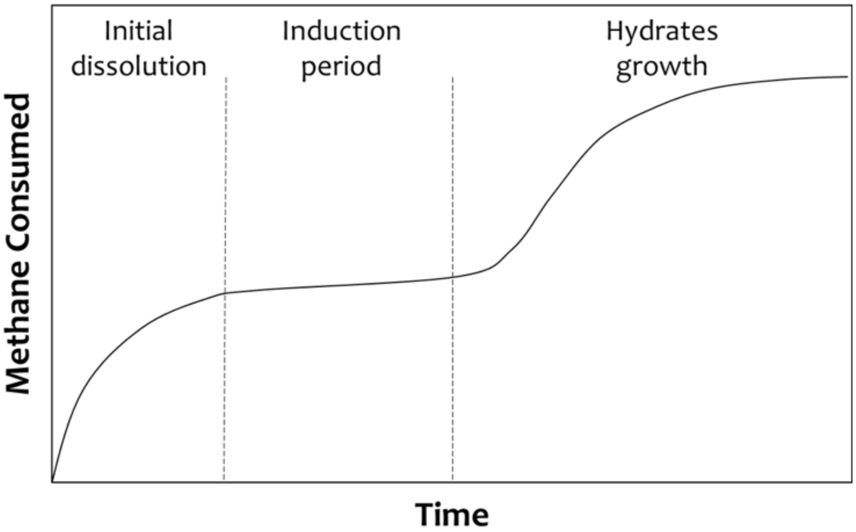

Figure 2. Three typical stages of methane consumption versus time during the hydrate formation process.

3. Promotion Factors

3.1 Nanostructures as Promoters

Researchers have conducted experiments at different thermodynamic conditions to study the promotion effects of the addition of nanostructures to the liquid phase participating in a hydration reaction. The criteria involved in the nanostructure selection are 1) the enhancement of heat transfer in the reactor and 2) providing more active heterogeneous sites for the nucleation step of hydrates. The mechanism of the improvement is based on the above criteria: the presence of the heterogeneous active sites promotes the nucleation step. Nanomaterials have a high surface/volume ratio and therefore, a small quantity of them provides numerous sites for the initiation of nucleation. The presence of a large number of sites not only decreases the induction time but also facilitates the formation of a larger quantity of hydrates that yields an increased storage capacity. Furthermore, certain nano particles can increase the heat transfer coefficient when added to water and this improvement in heat transfer is favored in the hydrate formation process. The hydration reaction is exothermic and the speeding of the purging of the released heat in the reactor accelerates the reaction. Although the reaction can be carried out at various combinations of pressures and temperatures, lower pressures and higher temperatures are more favorable. So far, the effect of a wide range of carbon nanostructures has been studied. Briefly, single [45] and multi-walled carbon nanotubes (CNT) [40, 46-51], graphene, graphene oxide[46], reduced graphene oxide [46], graphite nanoparticles [52, 53] as well as polymer coated [42] and metal nanoparticles grafted carbon nanotubes [41] have been studied, while the effect of fluorine on the formation of methane hydrates has never been investigated and there is a vacancy for a generic study on the effect of different morphologies of carbon nanostructures on methane hydrate formation process. On the other hand, other nanoparticles such as silver (Ag) [54, 55], copper (Cu) [56], titanium dioxide (TiO_2) [57], silicon dioxide (SiO_2) [58-60], Iron (II,III) oxide ($Fe3O_4$) [61], TiO2-Ag-SiO_2 sol [59], Zinc oxide (ZnO) [62] and Cupric oxide (CuO) [60, 63] have also been shown to promote the formation of methane hydrates. Nonetheless, the promotion effect of metal alloy nanoparticles is yet to be discovered.

3.2 Stabilization of Nanostructure Materials in Water

One of the challenging stages of using promoters in the hydrate formation process is the stabilization of the promoter in water. Although this is not an issue in the case of surfactants since they are mainly soluble in water, stabilization is of great importance for nanostructured materials as they tend to aggregate due to their high surface energy. This aggregation lowers the active surface of the nanoparticles and therefore, is unfavorable. Researchers have adopted common nanoparticle stabilization strategies to overcome this challenge. Sodium dodecyl sodium sulfate (SDS) surfactant has been widely used to stabilize TiO_2 [57], Fe_3O_4 [61], CuO [63], graphite, graphene, and other carbon nanostructures in water [49, 53, 64]. Other surfactants such as tetrahydrofuran (THF) have also been used [47]. Coating amphiphilic poly (styrene-co-sodium styrene sulfonate) copolymer on multi-wall carbon nanotubes has been proven to be another method to make a stable dispersion, where the copolymer/CNT mass ratio plays an important role and when increased up to 20, not only does it stabilize CNT in water, but also promotes the hydrate formation effectively [42]. Oxidation of carbon nanostructures is another method to make their surface hydrophilic. This can be either done by chemical oxidation of the surface [50], or synthesis of oxidized state directly [65].

3.3 Induction Time

Induction time is the period that a supersaturated metastable condition can withstand before it begins to form hydrates. This is relatively a long period and usually dominates the overall process time. Yang et al. stabilized a range of concentrations of graphite in water and studied its promotion at a range of pressure between 6.1 MPa to 9 MPa at 1 ^{o}C [53]. They showed that the optimum promotion occurs with a 0.4 wt% solution and the increase of pressure lowers the induction time up to 16 minutes. This data is almost consistent with other's group outcomes on investigating the effect of the same nanostructure. Lu et al. illustrated that at the elevated temperature of 4 ^{o}C, the maximum promotion is seen at 0.5 wt%, where the minimum induction time is 37 minutes [52]. Arjang et al. showed that the addition of silver nanoparticles in the absence of a surfactant can decrease the induction time up to 71.4 min, which is an 85% improvement compared to pure water [54]. They reported that this enhancement was due to three reasons: 1) the creation of a nanofluid with a higher heat transfer coefficient that facilitates the heat transfer in the reactor, 2) lowering the work required for hydrate nucleation in the presence of nano-sized heterogeneous nucleation sites and 3) the high surface-to-volume ratio in nonmetric particles providing a greater number of active sites. Another study on triangular silver nanoparticles showed that the induction time depends on the temperature and pressure at which the hydrates form [55]. They demonstrated that the increase in reactor pressure and reduction of reactor temperature favors the reduction of induction time. On the other hand, the increase in the concentration of silver nanoparticles from 4.5 to 27 µM decreases the induction time, while no further improvement was observed beyond 27 µM. The lowest induction time achieved was 5.04 min when 27 µM silver nanoparticles/water in a reactor charged with methane at 5.5 MPa at 2 ^{o}C was used. Copper nanoparticles have also been studied due to their enhancement in heat transfer within the reactor. The effectiveness of Cu nanoparticles in the presence and absence of CTAB was evaluated. Researchers illustrated that the addition of Cu nanoparticles in the absence of CTAB has a better promotion effect and the induction time can be lowered to 14 minutes [56]. This behavior may be attributed to the low contact angle between copper and water that facilitates the nucleation of hydrates. The promotion effect of SO_3^- coated carbon nanostructures has been well studied. It has been demonstrated that the use of SO_3^- coated graphene oxide can eliminate the induction time at the concentration of 750 ppm [64]. However, the use of 1 mM of SO_3^- grafted polystyrene nanospheres cannot exert that high level of effect, while the same nanoparticle with grafting COO and $N[CH_3]_3^+$ instead of SO_3^- is able to eliminate the induction time [66]. The efficacy of carbonated groups has also been confirmed elsewhere [67]. Wang et al. coated SO_3^- on polystyrene nanospheres and measured its efficacy in reducing the induction time, but the nanoparticles were unable to remarkably reduce this period, ending up no less than 80 minutes although the storage capacity was significantly improved[64, 68]. However, when they grafted Ag nanoparticles on SO_3^- coated polystyrene nanoparticles, they found that the induction time can be lowered to 17.8 minutes using this promoter [64]. This finding validates the promotion property due to the nanometric active nucleation site. They also showed that when SDS, CTAB, and dodecyl alcohol ethoxylates (AEO) are fixed on polystyrene nanoparticles, the induction time considerably drops [69]. The maximum improvement in the storage capacity and induction time was achieved with 8 mM of the SDS fixed on polystyrene nanoparticles in water, where the induction time declined to 12 minutes. The addition of more than 100 ppm of a high-density amphiphilic copolymer coated multi-wall CNT to water has been reported to eliminate the induction time, and hydrate clathrates can completely grow to reach equilibration in only 100 minutes [42]. Nonetheless, when Ag and Cu nanoparticles were grafted onto the CNTs, the reaction was completed in 125.1 and 141.8 respectively, though the induction time was still eliminated [41]. Nashed et al.

reported a consistent result in which the induction time was only one minute when CNTs were stabilized using SDS [48]. Another group reported that the induction time in the presence of smaller diameter-CNTs could be approximately 13 minutes [50]. These findings on the effect of the size of the nanostructure are completely consistent with Nesterov et al.'s findings [67]. Another group investigated the promotion effect of 1 wt% graphene sheets in hydrate formation of natural gas and found that the induction time can be reduced to 31 minutes [44]. On the contrary, the induction time was not significantly reduced when Hummers graphene oxide was used. Ghozatloo et al. reported that to be 161 minutes [65]. However, the induction time of the natural gas hydrate formation process in the presence of 1 wt% single-wall CNT has been reported to be as low as 15 minutes [45]. Investigation on the promotion effects of graphene, reduced graphene oxide, and multi-CNT at the freezing point of water further validated the previous results, where the induction time was dropped to only one minute when 360 ppm or 180 ppm of reduced graphene oxide/SDS and graphene oxide were used respectively, while the minimum induction time in the presence of multi-wall CNT was 3 minutes [46]. Although these results are in agreement with previous work on multi-wall CNTs [48, 50], the reason for reaching a significantly lower induction time compared to the natural gas mediated hydrate formation process can be attributed to the use of pure methane and also the difference in hydrate formation temperatures. Nesterov et al. investigated the use of silica, alumina, titania, zinc oxide, and magnesium oxide nanoparticles in the hydrate formation process of natural gas and found that magnesium oxide demonstrates the best performance amongst all of the metallic oxides tested, and the induction time was decreased to 32 minutes [67]. They also reported that the use of extremely small nanoparticles is not favored and that the nanoparticles with relatively larger sizes can promote the process more effectively. Pahlavanzadeh et al. investigated the addition of various concentrations of Al_2O_3, SiO_2, and CuO nanoparticles into pure water and illustrated that the minimum period of induction time occurs at 0.3 wt% of each dispersion and is 14, 18, and 13 minutes respectively. Another group confirmed the selection of 0.3 wt% as the maximum promotion of SiO_2, while the induction time is decreased to 17 minutes [58]. Govindaraj et al. also reported that the induction in the presence of silica nanoparticles can be as low as 13.2 minutes, further confirming the previous results [70]. Results obtain by Pahlavanzadeh et al. agree with the study of another group on CuO spherical nanoparticles. Aliabadi et al. stabilized various concentrations of CuO in water using SDS and elucidated that the maximum enhancement of the hydrate formation process happens when 10 ppm of the nanoparticle is used [63]. The minimum induction period recorded was 14 minutes, which was 92.7% less than that of pure water. Another research illustrated that the increase in CuO nanoparticle concentration up to 1 wt% reduces the induction time to 2.1 minutes when methane is hydrated at a low temperature of 1.5 ^{o}C [71]. Zinc oxide nanoparticles have also been used in different concentrations, pressures, and temperatures. Abdi-Khanghah et al. [62] reported that the induction time can be as low as 4.68 minutes when 0.05 wt% of the ZnO nanoparticle is used. They also demonstrated that the induction time decreases sharply as the pressure increases or temperature decreases. Li et al. found that the maximum reduction in induction time is achieved when 1% TiO_2 is used [57]. They studied concentrations between 0.01 to 1.5 wt% and reported that the induction time can be reduced to 14 minutes when 1 wt% TiO_2 nanoparticles in water are used. This reduction was reported to be due to the lower surface tension of TiO_2 nanofluid compared with water. Liu et al. used 200-1600 ppm SDS coated Fe_3O_4 nanoparticles in water and delineated that when more than 400 ppm of this promoter is used, the induction time is completely faded and hydrates start to grow readily after initial dissolution [61]. Table 1 provides a summary of studies that used a nanostructure material as the promoter for the hydrate formation process of methane-based gases.

3.4 Storage Capacity

Storage capacity is the indicator of how much gas can hydrates contain. The maximum storage capacity for methane hydrates is believed to be 180 cm^3/cm^3. This parameter is highly important in the industrial processes given that it can directly affect the feasibility of incorporation. Yang et al. showed that the storage capacity can be increased up to 126.6 for hydrates formed at 6.1 MPa and up to 162.8 for hydrates formed at 9 MPa [53]. They reported the promotion effects are linked with the presence of well-dispersed active sites for nucleation as well as the presence of graphite as a heat carrier within the system. Lu et al. found that the maximum storage capacity of hydrates promoted with graphite nanostructure is 112.2 at 6 MPa and 4 ^{o}C [52]. The improvement of the storage capacity of hydrates in the presence of multi-wall CNTs has been well studied [40-42, 47-51, 72]. A study showed that when multi-wall CNTs are coated with copolymers to stabilize in water, they can improve the storage capacity up to 138 [42]. They also showed that these CNTs have a great recycling performance, to the point that they could get a storage capacity as high as 132 after eight cycles of formation/dissociation and subsequent recovering the nanomaterials. When Ag and Cu were grafted on oxidized CNTs, the storage capacity was increased to 153 and 148.3 when formed in the presence of 10 ppm Ag/CNT and 20 ppm Cu/CNT dispersions respectively [41]. Another study also revealed that the addition of 30 ppm Multi-wall CNTs to THF/water solution can raise the amount of hydrated methane by 520% [47]. Hydroxylated and carboxylated multi-wall CNTs also effectively improve the storage capacity, increasing this value up to 163.7 [48], while the unfunctionalized multi-wall CNTs stabilized with reactive red 195 raised the storage capacity to 140 [51]. These findings suggest that the use of CNTs significantly increases the storage capacity of methane hydrates given the enhanced heat transfer of their nanofluid. Ganji et al. studied the effect of different concentrations of two types of nanoclays stabilized by different polymers and found that the storage capacity of hydrates formed at a severe 9.65 MPa and 2 ^{o}C surged to 179, which is extremely close to the theoretical value [6]. This promotion in storage was achieved when 500 ppm poly vinyl alcohol was used individually, while the hydrates were not the most stable among other samples. However, when they used 500 ppm Synthetic nanoclay laponite, the storage capacity raised to 167, and the stability improved drastically. Another study demonstrated that when 1 wt% graphene is introduced to the reaction at an elevated 4 ^{o}C, it can raise the storage capacity of natural gas hydrates to 133.7 [44]. In contrast, Hummer's graphene oxide barely showed any improvement in storage capacity, increasing the storage capacity only up to 92.6 [65]. Nevertheless, The addition of 1 wt% single-wall CNTs was able to increase it up to 161.7 [45]. Another study tested different oxide nanoparticles and reported that the MgO can surge the amount of hydrated natural gas more than three times [67]. The stabilization of nanostructures using hydrophilic groups, instead of surfactants, has also been investigated. Wang et al. showed that coating SO_3^- group on graphene oxide and using 750 g/L of its water solution can increase the storage capacity up to 143.9 [64]. The promotion made by silver nanoparticles grafted on SO_3^- coated polystyrene nanoparticles significantly influenced the storage capacity of methane hydrates, increasing it to 151.3 [64, 73]. Another study also proved that the grafting of hydrophilic groups such as COO and $N[CH_3]_3^+$ in conjunction with SO_3^- can increase the storage capacity up to 145 [66]. These studies reported that the superiority of this stabilization strategy is that it impedes the foaming effect resulting from SDS and hydrates form in a denser state. The dispersion of 0.3 wt% Al_2O_3, CuO, and SiO_2 in water was able to enhance the methane uptake 52.7%, 33%, and 59% respectively [60]. Another study further validated their results, where 10 ppm of CuO spherical nanoparticles increased the storage capacity by 34%[63]. Najibi et al. also confirmed the promotion achieved using CuO nanoparticles and calculated the storage capacity as high as 177 [71]. A study on ZnO nanoparticles revealed that the use of zinc oxide nano particles can almost double the amount of methane consumed [62]. Furthermore, Li et al. reported that TiO_2 nanoparticles can hardly improve the storage capacity of methane hydrates [57], but their pressure-time curved showed a great decrease in the reactor pressure over time compare to pure water, suggesting a massive increase in storage capacity.

Table 1. A summary of nanostructure materials that have been used in the hydrate formation process.

Promoter	Ave. Diameter (nm)	concentration	Reaction condition	Stabilizer	Group
Graphite nanoparticles	20	0.1 – 1 wt%	6.1 - 9 MPa @ 1 ^{o}C	SDS	Yang et al. [53]
	< 500	0.2-1 wt%	6 MPa @ 4 ^{o}C	SDS	Lu et al. [52]
Multi-wall CNT	8	10 – 150 ppm	6 MPa @ 2 ^{o}C	Poly (styrene-co-sodium styrene sulfonate)	Song et al. [42]
	8	100 ppm	6 MPa @ 2 ^{o}C	Reactive red 195	Song et al. [51]
Multi-wall CNT Oxidized Multi-wall CNT	8-15	0.1 wt%	6 MPa @ 2 ^{o}C	SDS	Song et al. [50]
Multi-wall CNT Carboxylated CNT Hydroxilated CNT	20 - 30	0.005 - 1 wt%	5.1 MPa @ 1 ^{o}C	SDS	Nashed et al. [48]
TiO2 nanoparticles	21	0.01 – 1.5 wt%	6 MPa @ 2 ^{o}C	SDS	Li et al. [57]

Graphene	-	1 wt%	6.8 MPa @ 4 °C	SDS	Hosseini et al. [44]
Graphene oxide Hummers	-	0-1 wt%	6.8 MPa @ 4 °C	-	Ghozatloo et al. [65]
Graphene oxide Reduced graphene oxide Milti-Wall CNT	-	90 - 540	4.5 MPa @ 0 °C	SDS Polyvinylpyrrolidone	Abedi‐ Farizhendi et al [46]
Sodium Montmorillonite nanoclay Synthetic nanoclay laponite	-	33 - 500 ppm	9.65 MPa @ 4 °C	Sulfonated polyacrylamide Poly vinyl alcohol Starch	Ganji et al. [6]
Single Wall-CNT	2	1 wt%	6 MPa @ 2 °C	SDS	Ghozatloo et al. [45]
Silver nanoparticles	50 - 75	0.27 wt%	4.7 and 5.7 MPa @ 2 °C	trisodium citrate	Arjang et al. [54]
	14.6	4.5 - 36 µmol/L	4.5 - 5.5 MPa @ 2 – 3 °C	trisodium citrate	Rahmati-Abkenar et al. [55]
Copper nanoparticles	25 - 75	0.0157 – 0.157 mol/L	5.5 MPa @ 2 °C	CTAB	Pahlavanzadeh et al. [56]
SO_3^- coated graphene oxide nanosheets	-	250 - 750 ppm	6 MPa @ 2 °C	-	Wang et al. [64]
SO_3^- coated polystyrene nanospheres	64	0.5 - 2 mmol/L	6 MPa @ 2 °C		Wang et al. [74]
Silver nanoparticles on SO_3^- coated polystyrene nanospheres	Ag: 2-5 Total: 108.7	0.1 - 0.5 mmol/L	6 MPa @ 2 °C	-	Wang et al. [64, 73]
Polystyrene nanospheres	40 - 110	1 - 8 mmol/L	6 MPa @ 2 °C	Fixation of SDS, CTAB and AEO on nanoparticles	Wang et al. [69]
Polystyrene nanospheres	40 - 200	1 mmol/L	6 MPa @ 2 °C	Grafting SO_3^-, COO and $N[CH_3]_3^+$	Lin et al. [66]
Ag and Cu nanoparticles-grafted Oxidized Multi-wall CNT	CNT: 8 Ag and Cu: Irregular	10 - 40 ppm	6 MPa @ 2 °C	Oxidation	Song et al. [41]
SDS coated Fe_3O_4 nanoparticles	20	200-1600 ppm	6 MPa @ 2 °C	SDS	Liu et al. [61]
Al_2O_3 nanoparticles SiO_2 nanoparticles CuO nanoparticles	15 15 < 50 nm	0.1 - 0.5 wt%	5.5 MPa @ 1 °C	-	Pahlavanzadeh et al. [60]
SiO_2 NPs Al_2O_3 NPs TiO_2 NPs ZnO NPs MgO NPs	30.6 – 31 12 – 34.4 13.8 261.4 79.8	1.2 wt%	8 MPa @ 0.5 °C	-	Nesterov et al. [67]
CuO nanoparticles	-	0.01 - 1 wt%	3.5 - 5.5 MPa @ 2.5 °C	SDS	Aliabadi et al. [63]
	40	0.01 - 1 wt%	5-6 MPa @ 1.5 - 4.5 °C	SDS	Najibi et al. [71]
SiO_2 nanoparticles	20 - 30	0.1 - 0.4 wt%	6 MPa	-	Cheng et al. [58]

			@ 1 ^{o}C		
	15	0.5 - 2 wt%	8 MPa @ 2 ^{o}C	-	Govindaraj et al. [70]
ZnO nanoparticles	10 - 30	0.05 - 0.1 wt%	5 - 6 MPa @ 1 - 3 ^{o}C	SDS	Abdi-Khanghah et al.

3.5 Stability

The stability of hydrates is ranked third among the most challenging obstacles. Although few projects have taken it under study, results suggest that wise selection of nano-promoters can increase the stability of hydrates formed as well. Figure 3 depicts a general trend of the dissociation of hydrates formed using pure water and its comparison with the use of stability-promoting nanostructures. Although hydrates begin to dissociate with time, the dissociation process stops when the self-preservation phenomenon dominates, and after that, no further hydrate is dissociated. Nanostructures are expected to reduce not only the amount of dissociation but also the time needed to reach self-preservation. Ganji et al. found that the addition of 500 ppm Synthetic nanoclay laponite can enormously increase the stability of methane hydrates, to the point that hydrates were completely stable after 24 hours at atmospheric pressure [6]. It has been shown that the use of only 1% wt graphene can limit the decomposition of natural gas hydrates up to 11.8% after 10 hours [44], while only 7.1% of the hydrates decomposed in the presence of single-wall CNT within the same period [45]. Despite the moderately improved stability of graphene and single-wall CNTs, Hummer's graphene oxide demonstrated a high level of stability, decomposing only 4.15% in 10 hours [65]. The authors reported that the elevated stability is due to the absence of any surfactant for the stabilization of this nanostructure in water. Their assertion can be justified because 1) hydrates are formed in the presence of SDS are made of small clusters, making fine hydrates [75], and 2) the volume to surface ratio is higher [48], which is due to the foaming of SDS/water solution [76]. A study on the stability of hydrates formed in the presence of carboxylated multi-wall CNTs also showed that although the hydrates formed using this promoter are more stable than that of SDS, hydrates are more prone to dissociation compared to those formed by pure water [48].

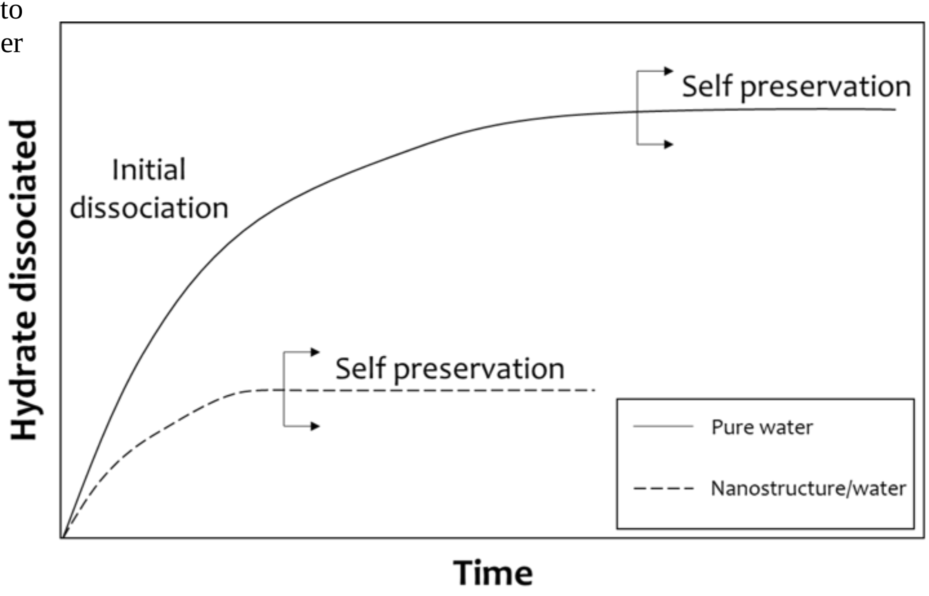

Figure 3. The typical trend of hydrate dissociation versus time. Nanostructure promoters are expected to increase the stability while decreasing the time needed to reach self-preservation.

4. Conclusions

The use of natural gas has been increased within the past decade. The current technologies for natural gas storage and transmission could be replaced with natural gas hydrate (NGH) technology to override several obstacles. However, the hydrate formation process needs to be promoted to maximize its potency. One solution is to use a nanofluid instead of water in the hydrate formation reaction. In this article, the promotion effect of nanostructured materials on the hydrate formation process of methane and natural gas was reviewed. It was found that nanopromoters, when correctly selected, are generally able to exhibit a notable improvement compared to pure water or a surfactant/water solution. The addition of small amounts of nanostructures to water has been able to reduce the induction time while increasing the storage capacity and stability of hydrates. The improvement obtained by the introduction of nanostructures is generally attributed to the presence of a large number of active sites that reduce the induction time and contribute to the generation of a large number of hydrates. These materials are specifically selected such that a nanofluid with an elevated heat transfer coefficient is obtained when a small quantity of these materials is added to water. It has been demonstrated that the increase in nanomaterial concentration does not necessarily improve the process and the optimum concentration should be found. Furthermore, although the nanoscale of the particle is favorable in the process, extremely small nanoparticles may not be as effective as regular nanoparticles. Despite many projects on the storage capacity and induction time of hydrates, very few have focused on the improvement of stability, therefore the stability study of hydrates is suggested to be included in future studies. Until now, a variety of nanostructures have been employed in the methane hydrate formation process such as metals and their oxide nanoparticles, polymer nanoparticles, and carbon nanostructure materials. Even though the promotion of different types of carbon nanostructures have been investigated, fullerene as the 0D state of carbon nanostructures has never been used, while it is expected to demonstrate promising results. Additionally, a generic study is needed to provide insights on the effect of the morphology of nanostructured materials on the challenges tied with the methane hydrate formation process. Metal alloy nanoparticles are also expected to demonstrate promising results and their effects on hydrate formation promotion need to be studied.

Acknowledgement

The author thanks Dr. Huiyuan Zhu and Katrina Avery for their help in the preparation of the paper.

Conflict of Interest

The authors declare that they have no conflict of interest.

References

[1] P. G. Lafond, K. A. Olcott, E. D. Sloan, C. A. Koh, and A. K. Sum, "Measurements of methane hydrate equilibrium in systems inhibited with NaCl and methanol," The journal of chemical thermodynamics, vol. 48, pp. 1-6, 2012.

[2] Y. Seo and S.-P. Kang, "Inhibition of methane hydrate re-formation in offshore pipelines with a kinetic hydrate inhibitor," Journal of Petroleum Science and Engineering, vol. 88, pp. 61-66, 2012.

[3] A. Demirbas, Methane gas hydrate: as a natural gas source. Springer, 2010.

[4] T. Collett *et al.*, "Methane Hydrates in Nature. Current Knowledge and Challenges," Journal of chemical & engineering data, vol. 60, no. 2, pp. 319-329, 2015.

[5] E. Chaturvedi, N. Prasad, and A. Mandal, "Enhanced formation of methane hydrate using a novel synthesized anionic surfactant for application in storage and transportation of natural gas," Journal of Natural Gas Science and Engineering, vol. 56, pp. 246-257, 2018.

[6] H. Ganji, J. Aalaie, S. Boroojerdi, and A. R. Rod, "Effect of polymer nanocomposites on methane hydrate stability and storage capacity," Journal of Petroleum Science and Engineering, vol. 112, pp. 32-35, 2013.

[7] Z. Liu, Z. Pan, Z. Zhang, P. Liu, L. Shang, and B. Li, "Effect of porous media and sodium dodecyl sulphate complex system on methane hydrate formation," Energy & fuels, vol. 32, no. 5, pp. 5736-5749, 2018.

[8] J. Javanmardi, K. Nasrifar, S. Najibi, and M. Moshfeghian, "Economic evaluation of natural gas hydrate as an alternative for natural gas transportation," Applied Thermal Engineering, vol. 25, no. 11-12, pp. 1708-1723, 2005.

[9] W. Hao, J. Wang, S. Fan, and W. Hao, "Evaluation and analysis method for natural gas hydrate storage and transportation processes," Energy conversion and management, vol. 49, no. 10, pp. 2546-2553, 2008.

[10] G. Rehder *et al.*, "Methane hydrate pellet transport using the self-preservation effect: a techno-economic analysis," Energies, vol. 5, no. 7, pp. 2499-2523, 2012.

[11] V. V. Nikitin *et al.*, "Dynamic in-situ imaging of methane hydrate formation and self-preservation in porous media," Marine and Petroleum Geology, vol. 115, p. 104234, 2020.

[12] R. Gilpin, "A study of factors affecting the ice nucleation temperature in a domestic water supply," The

Canadian Journal of Chemical Engineering, vol. 56, no. 4, pp. 466-471, 1978.

[13] A. Vysniauskas and P. Bishnoi, "A kinetic study of methane hydrate formation," Chemical Engineering Science, vol. 38, no. 7, pp. 1061-1072, 1983.

[14] D. Bai, X. Zhang, G. Chen, and W. Wang, "Replacement mechanism of methane hydrate with carbon dioxide from microsecond molecular dynamics simulations," Energy & Environmental Science, vol. 5, no. 5, pp. 7033-7041, 2012.

[15] P. M. Rodger, "Methane hydrate: melting and memory," Annals of the New York Academy of Sciences, vol. 912, no. 1, pp. 474-482, 2000.

[16] A. Demirbas, M. Rehan, B. O. Al-Sasi, and A.-S. Nizami, "Evaluation of natural gas hydrates as a future methane source," Petroleum Science and Technology, vol. 34, no. 13, pp. 1204-1210, 2016.

[17] Z. R. Chong, S. H. B. Yang, P. Babu, P. Linga, and X.-S. Li, "Review of natural gas hydrates as an energy resource: Prospects and challenges," Applied energy, vol. 162, pp. 1633-1652, 2016.

[18] B. C. Knott, V. Molinero, M. F. Doherty, and B. Peters, "Homogeneous nucleation of methane hydrates: Unrealistic under realistic conditions," Journal of the American Chemical Society, vol. 134, no. 48, pp. 19544-19547, 2012.

[19] Z.-g. Sun, R. Wang, R. Ma, K. Guo, and S. Fan, "Natural gas storage in hydrates with the presence of promoters," Energy Conversion and Management, vol. 44, no. 17, pp. 2733-2742, 2003.

[20] P. Di Profio, S. Arca, R. Germani, and G. Savelli, "Novel nanostructured media for gas storage and transport: clathrate hydrates of methane and hydrogen," 2007.

[21] A. Kumar, G. Bhattacharjee, B. Kulkarni, and R. Kumar, "Role of surfactants in promoting gas hydrate formation," Industrial & Engineering Chemistry Research, vol. 54, no. 49, pp. 12217-12232, 2015.

[22] H. I. Pérez-López, O. Elizalde-Solis, J. R. Avendaño-Gómez, A. Zúñiga-Moreno, and F. Sanchez-Minero, "Methane Hydrate Formation and Dissociation in Synperonic PE/F127, CTAB, and SDS Surfactant Solutions," Journal of Chemical & Engineering Data, vol. 63, no. 7, pp. 2477-2485, 2018.

[23] A. Fazlali, S. A. Kazemi, M. Keshavarz- Moraveji, and A. H. Mohammadi, "Impact of Different Surfactants and their Mixtures on Methane- Hydrate Formation," Energy Technology, vol. 1, no. 8, pp. 471-477, 2013.

[24] H. P. Veluswamy *et al.*, "Rapid methane hydrate formation to develop a cost effective large scale energy storage system," Chemical Engineering Journal, vol. 290, pp. 161-173, 2016.

[25] A. Kumar, N. Daraboina, R. Kumar, and P. Linga, "Experimental investigation to elucidate why tetrahydrofuran rapidly promotes methane hydrate formation kinetics: applicable to energy storage," The Journal of Physical Chemistry C, vol. 120, no. 51, pp. 29062-29068, 2016.

[26] D. Mech, P. Gupta, and J. S. Sangwai, "Kinetics of methane hydrate formation in an aqueous solution of thermodynamic promoters (THF and TBAB) with and without kinetic promoter (SDS)," Journal of Natural Gas Science and Engineering, vol. 35, pp. 1519-1534, 2016.

[27] Y. Qin *et al.*, "Formation and occurrence characteristics of methane hydrate in the complex system of sodium dodecyl sulfate and porous media," Energy Sources, Part A: Recovery, Utilization, and Environmental Effects, pp. 1-15, 2022.

[28] J. M. Lee, S. J. Cho, J. D. Lee, P. Linga, K. C. Kang, and J. Lee, "Insights into the kinetics of methane hydrate formation in a stirred tank reactor by in situ raman spectroscopy," Energy Technology, vol. 3, no. 9, pp. 925-934, 2015.

[29] N. Gnanendran and R. Amin, "Modelling hydrate formation kinetics of a hydrate promoter–water–natural gas system in a semi-batch spray reactor," Chemical engineering science, vol. 59, no. 18, pp. 3849-3863, 2004.

[30] W. Fu, Z. Wang, B. Sun, and L. Chen, "A mass transfer model for hydrate formation in bubbly flow considering bubble-bubble interactions and bubble-hydrate particle interactions," International Journal of Heat and Mass Transfer, vol. 127, pp. 611-621, 2018.

[31] Y. Qin, R. Bao, L. Shang, L. Zhou, and Z. Liu, "Growth and occurrence characteristics of methane hydrate in a complex system of silica sand and sodium dodecyl sulfate," Chem. Eng. Sci., vol. 249, p. 117349, 2022.

[32] Y. Qin *et al.*, "Effects of particle size and types of porous media on the formation and occurrence of methane hydrate in complex systems," Energy & Fuels, vol. 36, no. 1, pp. 655-668, 2021.

[33] L. Dongliang, P. Hao, and L. Deqing, "Thermal conductivity enhancement of clathrate hydrate with nanoparticles," International Journal of Heat and Mass Transfer, vol. 104, pp. 566-573, 2017.

[34] E. Andres-Garcia *et al.*, "Methane hydrates Nucleation in microporous materials," Chemical Engineering

Journal, vol. 360, no. 15, pp. 569-576, 2019.

[35] N.-J. Kim, J. H. Lee, Y. S. Cho, and W. Chun, "Formation enhancement of methane hydrate for natural gas transport and storage," Energy, vol. 35, no. 6, pp. 2717-2722, 2010.

[36] W. Liu, S. Wang, M. Yang, Y. Song, S. Wang, and J. Zhao, "Investigation of the induction time for THF hydrate formation in porous media," Journal of natural gas science and engineering, vol. 24, pp. 357-364, 2015.

[37] D. Kashchiev and A. Firoozabadi, "Nucleation of gas hydrates," Journal of crystal growth, vol. 243, no. 3-4, pp. 476-489, 2002.

[38] D. Kashchiev and A. Firoozabadi, "Induction time in crystallization of gas hydrates," Journal of crystal growth, vol. 250, no. 3-4, pp. 499-515, 2003.

[39] J. Parent and P. Bishnoi, "Investigations into the nucleation behaviour of methane gas hydrates," Chemical Engineering Communications, vol. 144, no. 1, pp. 51-64, 1996.

[40] J. Pasieka, S. Coulombe, and P. Servio, "Investigating the effects of hydrophobic and hydrophilic multi-wall carbon nanotubes on methane hydrate growth kinetics," Chemical Engineering Science, vol. 104, pp. 998-1002, 2013.

[41] Y.-M. Song, F. Wang, G. Guo, S.-J. Luo, and R.-B. Guo, "Energy-efficient storage of methane in the formed hydrates with metal nanoparticles-grafted carbon nanotubes as promoter," Applied Energy, vol. 224, pp. 175-183, 2018.

[42] Y.-M. Song, F. Wang, G. Guo, S.-J. Luo, and R.-B. Guo, "Amphiphilic-polymer-coated carbon nanotubes as promoters for methane hydrate formation," ACS Sustainable Chemistry & Engineering, vol. 5, no. 10, pp. 9271-9278, 2017.

[43] J. Carroll, Natural Gas Hydrates: A Guide for Engineers. Elsevier Science, 2009.

[44] M. Hosseini, A. Ghozatloo, and M. Shariaty-Niassar, "Effect of CVD graphene on hydrate formation of natural gas," Journal of Nanostructure in Chemistry, vol. 5, no. 2, pp. 219-226, 2015.

[45] A. Ghozatloo, N. M. Sharity, and M. Hassanisadi, "Effect of single walled carbon nanotubes on natural gas hydrate formation," Iranian Journal of Chemical Engineering, vol. 11, 3, pp. 67-73, 2014.

[46] S. Abedi-Farizhendi, M. Iranshahi, A. Mohammadi, M. Manteghian, and A. H. Mohammadi, "Kinetic study of methane hydrate formation in the presence of carbon nanostructures," Petroleum Science, vol. 16, no. 3, pp. 657-668, 2019.

[47] S. H. Lim, S. B. Riffat, S. S. Park, S. J. Oh, W. Chun, and N. J. Kim, "Enhancement of methane hydrate formation using a mixture of tetrahydrofuran and oxidized multi- wall carbon nanotubes," International journal of energy research, vol. 38, no. 3, pp. 374-379, 2014.

[48] O. Nashed, B. Lal, B. Partoon, K. M. Sabil, and Y. Hamed, "Kinematic Study of Methane Hydrate Formation and Self-Preservation in the Presence of Functionalized Carbon Nanotubes," Energy & Fuels, vol. 33, no. 8, pp. 7684-7695, 2019.

[49] J. Pasieka, S. Coulombe, and P. Servio, "The effect of hydrophilic and hydrophobic multi-wall carbon nanotubes on methane dissolution rates in water at three phase equilibrium (V− Lw− H) conditions," Industrial & Engineering Chemistry Research, vol. 53, no. 37, pp. 14519-14525, 2014.

[50] Y. Song, F. Wang, G. Liu, S. Luo, and R. Guo, "Promotion effect of carbon nanotubes-doped SDS on methane hydrate formation," Energy & Fuels, vol. 31, no. 2, pp. 1850-1857, 2017.

[51] Y.-M. Song, F. Wang, S.-J. Luo, R.-B. Guo, and D. Xu, "Methane hydrate formation improved by water-soluble carbon nanotubes via π-π conjugated molecules functionalization," Fuel, vol. 243, pp. 185-191, 2019.

[52] Y.-Y. Lu, B.-B. Ge, and D.-L. Zhong, "Investigation of using graphite nanofluids to promote methane hydrate formation: Application to solidified natural gas storage," Energy, p. 117424, 2020.

[53] L. Yang *et al.*, "Accelerated methane storage in clathrate hydrates using surfactant-stabilized suspension with graphite nanoparticles," Chinese Journal of Chemical Engineering, vol. 28, no. 4, pp. 1112-1119, 2020.

[54] S. Arjang, M. Manteghian, and A. Mohammadi, "Effect of synthesized silver nanoparticles in promoting methane hydrate formation at 4.7 MPa and 5.7 MPa," Chemical Engineering Research and Design, vol. 91, no. 6, pp. 1050-1054, 2013.

[55] M. Rahmati-Abkenar, M. Manteghian, and H. Pahlavanzadeh, "Experimental and theoretical investigation of methane hydrate induction time in the presence of triangular silver nanoparticles," Chemical Engineering Research and Design, vol. 120, pp. 325-332, 2017.

[56] H. Pahlavanzadeh, S. Rezaei, M. Khanlarkhani, M. Manteghian, and A. H. Mohammadi, "Kinetic study of methane hydrate formation in the presence of copper nanoparticles and CTAB," Journal of Natural Gas

Science and Engineering, vol. 34, pp. 803-810, 2016.

[57] X. Li, L. Sun, J. Jin, Y. Ding, and D. Jing, "Combined effects of surface tension and thermal conductivity on the methane hydrate formation in the presence of both nanoparticles and surfactant," Journal of Dispersion Science and Technology, 2019.

[58] Z. Cheng, Y. Zhao, W. Liu, Y. Liu, L. Jiang, and Y. Song, "Kinetic Analysis of Nano-SiO2 Promoting Methane Hydrate Formation in Porous Medium," Journal of Natural Gas Science and Engineering, p. 103375, 2020.

[59] J. D. Lee, H. C. Kim, Y. S. Kim, Y. D. Kim, and M. S. Lee, "Synthesis of nanosized TiO2-Ag-SiO2 sols by modified sol-gel method and their application for methane hydrate formation," in *solid state phenomena*, 2007, vol. 124: Trans Tech Publ, pp. 1059-1062.

[60] H. Pahlavanzadeh, M. Khanlarkhani, S. Rezaei, and A. H. Mohammadi, "Experimental and modelling studies on the effects of nanofluids (SiO2, Al2O3, and CuO) and surfactants (SDS and CTAB) on CH4 and CO2 clathrate hydrates formation," Fuel, vol. 253, pp. 1392-1405, 2019.

[61] G.-Q. Liu, F. Wang, S.-J. Luo, D.-Y. Xu, and R.-B. Guo, "Enhanced methane hydrate formation with SDS-coated Fe3O4 nanoparticles as promoters," Journal of Molecular Liquids, vol. 230, pp. 315-321, 2017.

[62] M. Abdi-Khanghah, M. Adelizadeh, Z. Naserzadeh, and H. Barati, "Methane hydrate formation in the presence of ZnO nanoparticle and SDS: Application to transportation and storage," Journal of Natural Gas Science and Engineering, vol. 54, pp. 120-130, 2018.

[63] M. Aliabadi, A. Rasoolzadeh, F. Esmaeilzadeh, and A. Alamdari, "Experimental study of using CuO nanoparticles as a methane hydrate promoter," Journal of Natural Gas Science and Engineering, vol. 27, pp. 1518-1522, 2015.

[64] F. Wang, H.-L. Meng, G. Guo, S.-J. Luo, and R.-B. Guo, "Methane hydrate formation promoted by− SO3–-coated graphene oxide Nanosheets," ACS Sustainable Chemistry & Engineering, vol. 5, no. 8, pp. 6597-6604, 2017.

[65] A. Ghozatloo, M. Hosseini, and M. Shariaty-Niassar, "Improvement and enhancement of natural gas hydrate formation process by Hummers' graphene," Journal of Natural Gas Science and Engineering, vol. 27, pp. 1229-1233, 2015.

[66] Y. Lin *et al.*, "Rapid formation of methane hydrates with compact agglomeration via regulating the hydrophilic groups of nanopromoters," AIChE Journal, vol. 66, no. 9, p. e16296, 2020.

[67] A. Nesterov *et al.*, "Promotion and inhibition of gas hydrate formation by oxide powders," Journal of Molecular Liquids, vol. 204, pp. 118-125, 2015.

[68] F. Wang, G. Guo, S.-J. Luo, and R.-B. Guo, "Preparation of–SO 3−-coated nanopromoters for methane hydrate formation: effects of the existence pattern of–SO 3− groups on the promotion efficiency," Journal of Materials Chemistry A, vol. 5, no. 6, pp. 2640-2648, 2017.

[69] F. Wang, G.-Q. Liu, H.-L. Meng, G. Guo, S.-J. Luo, and R.-B. Guo, "Improved methane hydrate formation and dissociation with nanosphere-based fixed surfactants as promoters," ACS Sustainable Chemistry & Engineering, vol. 4, no. 4, pp. 2107-2113, 2016.

[70] V. Govindaraj, D. Mech, G. Pandey, R. Nagarajan, and J. S. Sangwai, "Kinetics of methane hydrate formation in the presence of activated carbon and nano-silica suspensions in pure water," Journal of Natural Gas Science and Engineering, vol. 26, pp. 810-818, 2015.

[71] H. Najibi, M. M. Shayegan, and H. Heidary, "Experimental investigation of methane hydrate formation in the presence of copper oxide nanoparticles and SDS," Journal of Natural Gas Science and Engineering, vol. 23, pp. 315-323, 2015.

[72] N.-J. Kim, S.-S. Park, H. T. Kim, and W. Chun, "A comparative study on the enhanced formation of methane hydrate using CM-95 and CM-100 MWCNTs," International communications in heat and mass transfer, vol. 38, no. 1, pp. 31-36, 2011.

[73] F. Wang, Y.-M. Song, G.-Q. Liu, G. Guo, S.-J. Luo, and R.-B. Guo, "Rapid methane hydrate formation promoted by Ag&SDS-coated nanospheres for energy storage," Applied Energy, vol. 213, pp. 227-234, 2018.

[74] F. Wang *et al.*, "Methane hydrate formation with surfactants fixed on the surface of polystyrene nanospheres," Journal of Materials Chemistry A, vol. 3, no. 16, pp. 8316-8323, 2015.

[75] H. Cui, X. Yan, M. Monasterio, and F. Xing, "Effects of various surfactants on the dispersion of MWCNTs–OH in aqueous solution," Nanomaterials, vol. 7, no. 9, p. 262, 2017.

[76] H. P. Veluswamy, A. Kumar, Y. Seo, J. D. Lee, and P. Linga, "A review of solidified natural gas (SNG)

technology for gas storage via clathrate hydrates," Applied Energy, vol. 216, pp. 262-285, 2018.